Earth and Planetary Science Letters 425 (2015) 168–178

Contents lists available at ScienceDirect

Earth and Planetary Science Letters

www.elsevier.com/locate/epsl

Diffusive over-hydration of olivine-hosted melt inclusions

Margaret E. Hartley [a,b,*], David A. Neave [a], John Maclennan [a], Marie Edmonds [a], Thor Thordarson [c]

[a] Department of Earth Sciences, University of Cambridge, Downing Street, Cambridge, CB2 3EQ, UK
[b] School of Earth, Atmospheric and Environmental Sciences, University of Manchester, Oxford Road, Manchester, M13 9PL, UK
[c] Institute of Earth Sciences, University of Iceland, Sturlugata 7, 101 Reykjavík, Iceland

ARTICLE INFO

Article history:
Received 17 March 2015
Received in revised form 15 May 2015
Accepted 3 June 2015
Available online 11 June 2015
Editor: B. Marty

Keywords:
melt inclusion
melt mixing
diffusion
water
olivine
Iceland

ABSTRACT

The pre-eruptive water content of magma is often estimated using crystal-hosted melt inclusions. However, olivine-hosted melt inclusions are prone to post-entrapment modification by H^+ diffusion as they re-equilibrate with their external environment. This effect is well established for the case of H^+ loss from olivine-hosted inclusions that have cooled slowly in degassed magma. Here we present evidence for the opposite effect: the addition of H^+ into inclusions that are held in melts that are enriched in H_2O with respect to the trapped melts. The compositional variability in a suite of 211 olivine-hosted inclusions from the Laki and Skuggafjöll eruptions in Iceland's Eastern Volcanic Zone indicates that diffusive H^+ gain governs the H_2O content of incompatible trace element depleted inclusions. Individual eruptive units contain olivine-hosted inclusions with widely varying incompatible element concentrations but near-constant H_2O. Furthermore, over 40% of the inclusions have $H_2O/Ce > 380$, significantly higher than the H_2O/Ce expected in primary Icelandic melts or mid-ocean ridge basalts (150–280). The fact that the highest H_2O/Ce ratios are found in the most incompatible element depleted inclusions indicates that hydration is a consequence of the concurrent mixing and crystallisation of compositionally diverse primary melts. Hydration occurs when olivines containing depleted inclusions with low H_2O contents are juxtaposed against more hydrous melts during mixing. Melt inclusions from a single eruption may preserve evidence of both diffusive H^+ loss and H^+ gain. Trace element data are therefore vital for determining H_2O contents of melt inclusions at the time of inclusion trapping and, ultimately, the H_2O content of the mantle source regions.

1. Introduction

The water content of melt inclusions is commonly assumed to be a lower bound on the pre-eruptive H_2O content of melts stored in the crust (Métrich and Wallace, 2008). However, H_2O concentrations in olivine-hosted melt inclusions may be lowered, or more unusually, increased by post-entrapment diffusion of hydrogen through the host olivine as inclusions equilibrate with their external environment. Experimental studies have demonstrated that olivine-hosted melt inclusions with high initial H_2O contents are susceptible to diffusive dehydration on heating under dry external conditions, with diffusive H_2O loss occurring within hours to days at magmatic temperatures (e.g. Danyushevsky et al., 2002; Gaetani et al., 2012; Bucholz et al., 2013). Natural olivine-hosted inclusions in erupted lavas and tephras also illustrate this phenomenon, which may occur either during magma ascent or during thermally insulated transport in a degassed carrier melt (e.g. Massare et al., 2002; Chen et al., 2013; Lloyd et al., 2013; Le Voyer et al., 2014). Conversely, relatively dry melt inclusions are in theory susceptible to diffusive H^+ gain if they are stored in a water-rich carrier melt (Portnyagin et al., 2008), but this has seldom been demonstrated in nature (Koleszar et al., 2009).

Here we present evidence of both diffusive hydration and dehydration in a suite of naturally quenched olivine-hosted melt inclusions from Iceland's Eastern Volcanic Zone. Hydrated melt inclusions are depleted in incompatible trace elements: they have low values of trace element ratios such as La/Yb and Ce/Y, and anomalously high H_2O/Ce. This hydration of depleted melt inclusions is an inevitable consequence of concurrent mixing and crystallisation of diverse primary melt compositions. This is the first study to illustrate melt inclusion hydration due to water gradients set up by the mixing of melts with heterogeneous mantle parents. We use diffusion modelling to calculate the timescales of diffusive hydration and dehydration in these samples, and explore

* Corresponding author at: School of Earth, Atmospheric and Environmental Sciences, University of Manchester, Oxford Road, Manchester, M13 9PL, UK.
E-mail address: margaret.hartley@manchester.ac.uk (M.E. Hartley).

http://dx.doi.org/10.1016/j.epsl.2015.06.008

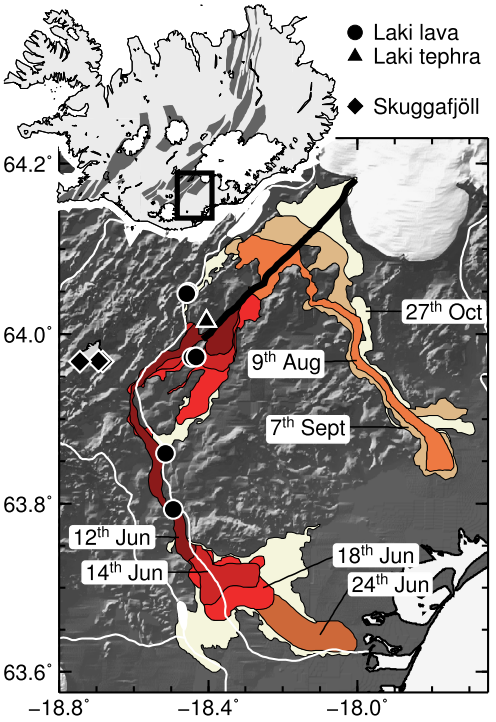

Fig. 1. Map of Iceland's Eastern Volcanic Zone, showing the locations of Skuggafjöll mountain and the AD 1783 Laki lava flow field. The 27 km-long Laki fissure is shown as a thick black line. The dates show the progress of flow emplacement as the Laki lava flowed from the source vents down river gorges towards the coastal plain. Flow boundaries and dates are reproduced after Thordarson and Self (1993). The locations of the samples discussed in this study are indicated by black symbols. Inset: map of Iceland, with neovolcanic zones shown in dark grey.

the timescales over which olivine-hosted inclusions can retain hydrated, high H_2O/Ce signatures. Finally, we demonstrate that hydration of depleted melt inclusions is not restricted to Iceland, but is a feature of many global melt inclusion datasets.

2. Samples

This study focuses on samples from the Laki and Skuggafjöll eruptions located in Iceland's Eastern Volcanic Zone (EVZ) (Fig. 1). The AD 1783–1784 Laki eruption produced 15.1 km^3 dense rock equivalent of lava and tephra, making this one of the largest basaltic fissure eruptions recorded in human history. The ~27 km-long Laki fissure erupted sequentially in 10 *en echelon* segments over a period of 8 months (Thordarson and Self, 1993). The samples consist of fresh magmatic tephra obtained from proximal fall deposits around the Laki cone row and quenched glassy lava selvages from sites around the Skaftá river gorge (Hartley et al., 2014). Skuggafjöll is an ~800 m-high mountain located towards the southern end of an NE–SW-striking hyaloclastite ridge that probably formed at >10 ka during the last glacial period (Neave et al., 2014a). The mountain comprises vesicular pillow lavas and intercalated hyaloclastites, all of which are highly phyric. The Skuggafjöll samples consist of glassy pillow basalts from localities near the base of the mountain.

Our dataset consists of major, trace and volatile elements measured in 97 olivine-hosted melt inclusions (70 from lava samples, 27 from tephra samples) and 19 glasses from Laki, and 114 olivine-hosted inclusions and 6 glasses from Skuggafjöll. The olivine macrocrysts were hand-picked from crushed samples and range in diameter from 450 to 1100 μm, while the melt inclusions range from 22 to 307 μm in diameter. Care was taken to select only naturally glassy melt inclusions containing no daughter crystals. Compositional data for the Laki and Skuggafjöll samples are taken from Hartley et al. (2014) and Neave et al. (2014a) respectively, where details of analytical methods and data reduction procedures can also be found. Trace element and H_2O concentrations in melt inclusions and glasses were analysed by secondary ion mass spectrometry (SIMS) at the University of Edinburgh. Precision and accuracy of SIMS analyses were monitored by repeat analyses of basaltic glass standards. 1σ precision was ±5% for trace elements of high abundance (e.g. La, Ce) and ±10 for trace elements of low abundance (e.g. Yb, Lu). 1σ accuracy for trace elements is estimated at ±10%. Precision and accuracy of H_2O measurements were estimated at ±4% for Laki samples and ±10% for Skuggafjöll samples. Major element compositions of glass, melt inclusions and their host olivines were analysed by electron microprobe (EPMA) at the University of Cambridge.

3. H_2O/Ce in Icelandic melt inclusions

Volatile-trace element pairs such as H_2O and Ce, or CO_2 and Nb or Rb, have similar bulk partition coefficients and are expected to exhibit similar geochemical behaviour during mantle melting and fractional crystallisation (e.g. Michael, 1995; Danyushevsky et al., 2000; Dixon and Clague, 2001; Saal et al., 2002; Rosenthal et al., 2015). This indicates that Ce can be used as a proxy for the initial undegassed H_2O content of a melt inclusion, provided that H_2O/Ce of the primary melt is known. This ratio can be determined by analysing undegassed melt inclusions or glasses, which are expected to show a strong positive correlation between H_2O and Ce. Global compilations of nominally undegassed mid-ocean ridge glasses display this correlation, and typically have H_2O/Ce between 150 and 280 (e.g. Michael, 1995; Danyushevsky et al., 2000; Saal et al., 2002; Naumov et al., 2014). There is no known correlation between H_2O/Ce and spreading rate, nor the extent or depth of melting (Michael, 1995). However, average H_2O/Ce values are known to differ between MORB samples from the Atlantic, Pacific and Indian oceans (Naumov et al., 2014); there are also significant regional variations between different ridge segments (Michael, 1995). This indicates that for any given region the value of H_2O/Ce is characteristic of the mantle source.

Our Laki and Skuggafjöll melt inclusions contain between 0.07 and 0.76 wt% H_2O (Hartley et al., 2014; Neave et al., 2014a), consistent with results from previous studies of EVZ melt inclusions and glasses (Métrich et al., 1991; Nichols et al., 2002). If these values represent vapour-undersaturated melt H_2O contents at the time of inclusion trapping during the crystallisation of a parental melt, then H_2O and Ce should correlate positively. However, no such correlation is observed (Fig. 2). EVZ inclusions and glasses have H_2O/Ce between 20 and 1103, and most analyses fall outwith the range of H_2O/Ce values expected for undegassed MORB glasses (Fig. 2). The data can be divided into three populations. Firstly, the Laki glass and melt inclusions from Laki lava samples have low H_2O and low H_2O/Ce over a range of Ce contents and host olivine compositions. Secondly, Skuggafjöll inclusions and some Laki tephra inclusions have low (~10 ppm) Ce and high H_2O/Ce, and are hosted in Fo > 82 olivines. Thirdly, the Skuggafjöll glass and the majority of inclusions from Laki tephra samples have H_2O/Ce within the expected range for undegassed MORB glasses.

4. H_2O and trace element variability in EVZ melt inclusions

In order to determine the cause of H_2O/Ce variability in the EVZ melt inclusions, it is necessary to identify the processes controlling H_2O and Ce concentrations in these inclusions. Here we explore the extent to which trace element concentrations and ratios can be explained by crystallisation, melt mixing, and boundary layer effects.

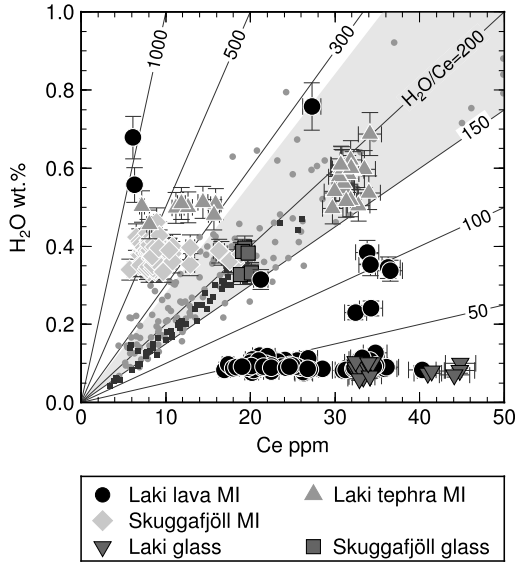

Fig. 2. H_2O vs. Ce for melt inclusions and glasses from Iceland's Eastern Volcanic Zone. Lines show contours of constant H_2O/Ce. Small symbols show H_2O and Ce concentrations for a global compilation of undegassed MORB glasses (light circles: Michael, 1995; dark squares: Danyushevsky et al., 2000). The grey shaded area shows the expected range in H_2O/Ce for undegassed MORB glasses of $150 < H_2O/Ce < 280$.

4.1. Fractional crystallisation

Reverse fractional crystallisation models were calculated for the Laki and Skuggafjöll magmas using Petrolog3 (Danyushevsky and Plechov, 2011). Starting compositions were the average tephra glass composition for Laki (Hartley et al., 2014), and the average quenched pillow glass composition for Skuggafjöll (Neave et al., 2014a). Calculations were performed at 0.001, 2, 4 and 6 kbar, reflecting the likely pressures of crystallisation within EVZ magmatic systems. Calculations used an fO_2 of one log unit below the QFM buffer and the mineral-melt equilibrium models of Danyushevsky (2001) for plagioclase, clinopyroxene and olivine, with $Kd^{ol\text{-}liq}_{Fe-Mg}$ modelled after Toplis (2005). Ce and Y were modelled as incompatible trace elements using the partition coefficients given in Table S1.

EVZ melt inclusions have typically experienced ≤2% post-entrapment crystallisation (PEC) of olivine on inclusion walls. The maximum extents of PEC for Laki and Skuggafjöll are 7% and 5% respectively (Hartley et al., 2014; Neave et al., 2014a). Melt inclusion Mg# [where Mg# = 100 × atomic Mg/(Mg + Fe)] is therefore unlikely to reflect the initial trapped melt composition. However, the ratio CaO/Na_2O remains largely unaffected by PEC since both Ca and Na are incompatible in olivine (Neave et al., 2013). A plot of melt inclusion CaO/Na_2O vs. Ce reveals that absolute Ce concentrations in both Laki and Skuggafjöll melt inclusions largely follow expected fractional crystallisation trends (Fig. 3(a)). This is supported by strong negative correlations between host olivine forsterite and melt inclusion Ce for both Laki and Skuggafjöll (Fig. S3). However, melt inclusion H_2O contents deviate significantly from the predicted fractional crystallisation trend (Fig. 3(b)).

There is considerable variability in melt inclusion Ce at a given CaO/Na_2O, especially for Laki (Fig. 3(a)). The melt inclusion compositions therefore cannot be modelled by simple fractionation of a parental melt along a single liquid line of descent. High CaO/Na_2O is associated with depleted primary melt compositions, while low CaO/Na_2O is associated with enriched primary melts: this has been demonstrated for Icelandic melts (Shorttle and Maclennan, 2011) as well as for mid-ocean ridge basalts (e.g. Elthon and Casey, 1985 and references therein). The scatter in Fig. 3(a) may therefore be explained by the concurrent crystallisation and mixing of heterogeneous primary melts.

4.2. Concurrent mixing and crystallisation

Melt inclusions from both Laki and Skuggafjöll record statistically significant decreases in ratios of highly incompatible to moderately incompatible trace elements, such as La/Yb or Ce/Y, as host olivine forsterite decreases (Neave et al., 2013; Neave et al., 2014a; Hartley et al., 2014). The Ce/Y variability in the EVZ melt inclusions cannot be explained by fractional crystallisation alone (Fig. 3(c)). La/Yb and Ce/Y are passive tracers of incompatible trace element enrichment in primary melts, and decreasing variability of these ratios with decreasing host forsterite content is indicative of concurrent mixing and crystallisation of diverse primary melts. This process has been well documented in Icelandic magmatic systems (Maclennan, 2008; Neave et al., 2013).

In order to compare simultaneously the compositional variations present in olivine-hosted melt inclusions from different eruptions, Maclennan (2008) defined the parameter Þ to be a measure

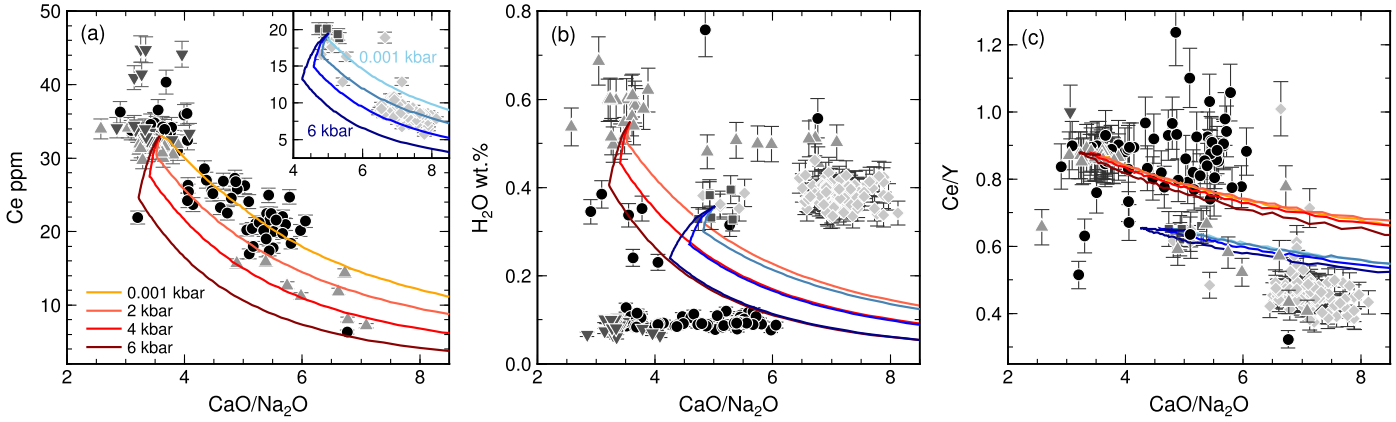

Fig. 3. (a) CaO/Na_2O vs. Ce for melt inclusions and matrix glasses from Laki and, inset, for Skuggafjöll, using the same symbols as Fig. 2. Coloured lines show reverse fractional crystallisation trends calculated over a range of pressures (see text for details). Starting compositions were the average tephra glass composition for Laki, and the average quenched pillow glass composition for Skuggafjöll. Glassy lava selvages from Laki have more evolved compositions and higher Ce concentrations than the Laki tephra, as a result of crystallisation during insulated transport within the Laki lava. (b) CaO/Na_2O vs. H_2O for EVZ melt inclusions and glasses. H_2O contents of Skuggafjöll and Laki tephra melt inclusions are much higher than predicted by fractional crystallisation trends. (c) CaO/Na_2O vs. Ce/Y for EVZ melt inclusions and glasses. Ratios of highly to moderately incompatible trace elements are widely scattered about the calculated fractional crystallisation trends. (For interpretation of the references to colour in this figure legend, the reader is referred to the web version of this article.)

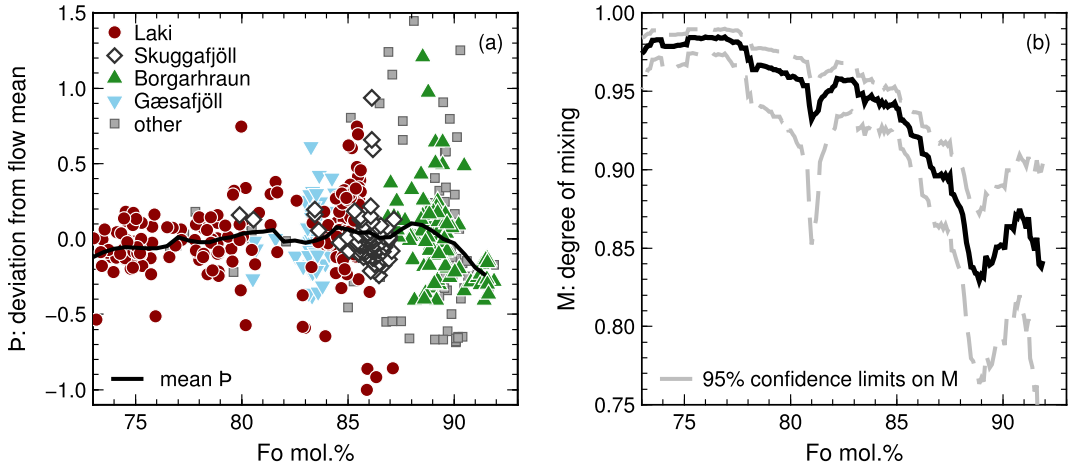

Fig. 4. The record of concurrent mixing and crystallisation in Iceland. (a) Plot showing the reduction in compositional variability of melt inclusions as host olivine forsterite decreases. The plot shows melt inclusions from Iceland as a whole, with different symbols highlighting different eruptions including Laki and Skuggafjöll. The mean melt inclusion Þ at a given host forsterite content is shown by the black solid line. (b) Variation in the extent of melt mixing, *M*, with olivine forsterite content. Grey lines show the 95% confidence interval of *M* at a given forsterite content. The parameters Þ and *M* are briefly described in the text and are fully discussed by Maclennan (2008).

of the deviation of a melt inclusion composition from the average composition of the eruption that it comes from, normalised to the expected standard deviation of the original, unmixed enriched and depleted endmember melt compositions for the eruption. On a plot of Þ vs. host olivine composition, melt inclusions from Laki and Skuggafjöll fall within the triangular envelope defined by previously studied Icelandic eruptions (Fig. 4(a); Gurenko and Chaussidon, 1995, 1997, 2002; Slater et al., 2001; Maclennan et al., 2003a, 2003b; Maclennan, 2008; Hartley and Thordarson, 2013; Neave et al., 2013). As melt mixing and crystallisation proceed, Þ converges towards zero. The extent of magma mixing, *M*, can then be calculated as a function of host olivine composition using melt inclusion Þ values. *M* ranges from zero for unmixed endmember primary melts to unity when mixing is complete (Maclennan, 2008). There is a sharp increase in *M* at an olivine composition of Fo_{88}, followed by a slower but steady increase as melts crystallise and host olivines evolve from Fo_{83} to Fo_{73} (Fig. 4(b)). The changes in *M* above Fo_{88} reflect the input of diverse primary melt compositions into magma reservoirs where crystallisation is occurring (Maclennan, 2008; Rudge et al., 2013). Mixing processes are dominant between Fo_{88} and Fo_{83}, and by Fo_{83} much of the mantle-derived heterogeneity has been erased. These calculations demonstrate that trace element concentrations and ratios in our EVZ melt inclusions can be successfully modelled by concurrent mixing and crystallisation of diverse mantle melts.

4.3. Boundary layer and dissolution effects

Incompatible element-enriched boundary layers form at the edges of rapidly growing crystals when the crystallisation rate exceeds the diffusion rate (e.g. Faure and Schiano, 2005). Melt inclusions that trap boundary layers therefore do not represent the composition of their parental melt. Natural olivines are surrounded by 1–3 μm-wide incompatible element-enriched boundary layers, but olivine-hosted inclusions with diameter >20 μm show almost no geochemical evidence of boundary layer trapping (Kuzmin and Sobolev, 2004). Melt inclusions <20 μm are therefore expected to be most affected by boundary layer entrapment, with negative correlations between melt inclusion size and incompatible element concentrations. At magmatic temperatures, H_2O diffuses sufficiently quickly through basaltic melt to prevent significant H_2O enrichment in boundary layers (Baker et al., 2005). Diffusion of Ce is very slow compared to diffusion of H_2O (Zhang and Ni, 2010; Zhang et al., 2010). Melt inclusions that trapped boundary layers might thus be expected to have elevated Ce concentrations and low H_2O/Ce. All but one of the EVZ inclusions have diameter >30 μm and there is no correlation between inclusion size and Ce content or H_2O/Ce (Fig. S5), indicating that boundary layer trapping is negligible in our dataset.

Boundary layers also form within melt inclusions during post-entrapment crystallisation. The centre of a melt inclusion will preserve the initial melt composition unless the leading edge of the propagating boundary layer reaches its centre. A critical radius therefore exists for each element, below which the composition at the inclusion centre will be influenced by PEC and diffusion in the melt, and above which the initial inclusion composition will be preserved (Newcombe et al., 2014). Small melt inclusions are more prone to compositional modification by internal boundary layers. While we cannot definitively rule out internal boundary layers in our EVZ melt inclusions, we note that the inclusions were cut as close to their centres as possible (which reduces the likelihood of sectioning the boundary layer); that EPMA and SIMS analyses were made close to inclusion centres; and that the critical radius for Ce is expected to be small ($\ll$50 μm) given its low diffusivity in basaltic melts (Zhang et al., 2010). Furthermore, previous studies have suggested that melt inclusion H_2O contents are more strongly affected by diffusion into/out of the inclusion through the host olivine than by internal boundary layer effects (Chen et al., 2013; Newcombe et al., 2014).

Dissolution–reaction-mixing (DRM) processes have been invoked as an explanation for trace element diversity in melt inclusions (e.g. Danyushevsky et al., 2003). Inclusions generated by DRM processes involving plagioclase are expected to have very low La concentrations, low La/Yb, and large positive Sr anomalies quantified by the parameter Sr/Sr*, where $Sr/Sr^* = Sr_n/(Ce_n \times Nd_n)^{0.5}$ and the subscript *n* indicates chondrite-normalised values. Average Sr/Sr* is 0.78 ± 0.21 (1σ) for Laki inclusions and 1.15 ± 0.16 (1σ) for Skuggafjöll inclusions. These low Sr/Sr* values indicate that DRM exerts no significant control over trace element variability in these inclusions. Compositions of plagioclase and clinopyroxene crystals and plagioclase-hosted melt inclusions support this interpretation (Neave et al., 2013; Neave et al., 2014b). Furthermore, Maclennan (2008) demonstrated that DRM processes alone cannot generate the range in trace element ratios such as La/Yb and Sm/Yb observed in Icelandic melt inclusions.

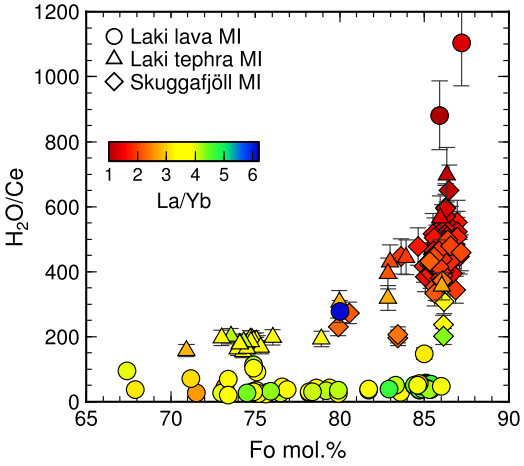

Fig. 5. Melt inclusion H_2O/Ce vs. host olivine composition, coloured by La/Yb. At high forsterite content there is a wide range in H_2O/Ce and La/Yb. As forsterite decreases, the variability in La/Yb collapses to the mean La/Yb of the eruption, and the variability in H_2O/Ce decreases. (For interpretation of the references to colour in this figure legend, the reader is referred to the web version of this article.)

5. Modification of H_2O/Ce through H^+ diffusion

The EVZ melt inclusions define a trend of decreasing H_2O/Ce with decreasing host forsterite content (Fig. 5). Inclusions in the most forsteritic olivines show the widest range in H_2O/Ce, but this quickly collapses such that inclusions hosted in Fo < 77 olivines have $H_2O/Ce < 210$. H_2O/Ce also correlates negatively with La/Yb. At high forsterite, the most depleted inclusions (La/Yb < 2) have the highest H_2O/Ce, while more enriched inclusions (La/Yb > 4) have lower H_2O/Ce. High H_2O/Ce in depleted melt inclusions is unlikely to be a primary feature, since this would require depleted melts to have significantly higher H_2O than enriched melts, despite their lower Ce contents. In addition, it cannot be explained by concurrent mixing and crystallisation of enriched and depleted primary melts alone: if H_2O and Ce behave as similarly incompatible trace elements and do not diffuse or degas, then the processes of mixing and crystallisation are not expected to fractionate H_2O from Ce. Concurrent mixing and crystallisation should produce suites of melt inclusions with approximately constant H_2O/Ce regardless of melt La/Yb or host olivine composition.

The observed H_2O/Ce variability in the EVZ inclusions is best explained by the diffusion of H_2O into or out of the melt inclusions as they equilibrate with their carrier melts. Hydrogen diffusion in olivine is complex and occurs via several mechanisms: protons may exchange with Mg vacancies (denoted [Mg]); Si or Ti vacancies, ([Si], [Ti]); trivalent cations; electronic defects (proton–polaron exchange, denoted 'PP'); or a combination of these mechanisms (e.g. Padrón-Navarta et al., 2014; Peslier et al., 2015). The diffusion rate is dependent on the diffusion mechanism(s): in general, $D_{[Si]} \ll D_{[Ti]+[Si]} < D_{[Mg]} < D_{PP}$, although at magmatic temperatures the diffusion coefficients for [Mg] and [Ti] + [Si] converge to similar values of $\sim 10^{-11}$–10^{-12} m^2/s (e.g. Demouchy and Mackwell, 2006; Padrón-Navarta et al., 2014). Both [Mg] and PP mechanisms are anisotropic (Mackwell and Kohlstedt, 1990; Demouchy and Mackwell, 2006), but anisotropy has not been reported for other diffusion mechanisms. The proton–polaron mechanism is also referred to as redox exchange, and is enhanced by oxidising conditions. However, recent studies of both natural and experimental samples indicate that at magmatic temperatures, H^+ diffusion independent of oxygen fugacity can modify H_2O concentrations in olivine-hosted melt inclusions by several weight percent on timescales of hours to days (Gaetani et al., 2012; Bucholz et al., 2013).

5.1. H_2O/Ce in Icelandic primary melts

In order to assess the extent of diffusive re-equilibration in the EVZ inclusions, H_2O/Ce must be determined for undegassed melts. Volatile saturation models indicate that the Skuggafjöll magma erupted under ice/water pressures of ~1.4 MPa (Neave et al., 2014a), which is sufficient to prevent significant H_2O degassing. The average H_2O/Ce of 184 ± 19 preserved in glassy pillow rims from Skuggafjöll is thus likely to represent the undegassed H_2O/Ce of the Skuggafjöll magma. Melt inclusions from the Laki tephra were rapidly quenched upon eruption, and are unlikely to have experienced post-eruptive H^+ loss. A subset of inclusions from the Laki tephra hosted in low forsterite olivines have La/Yb values that are identical within error to the Laki glass, indicating that these inclusions were trapped during late-stage crystallisation. The average H_2O/Ce of these inclusions, 182 ± 14, is expected to be representative of the pre-eruptive undegassed Laki magma.

While Skuggafjöll glass has a lower average La/Yb than Laki glass (2.60 compared to 3.82), the undegassed H_2O/Ce values for Laki and Skuggafjöll are identical within error. This suggests that enriched and depleted Icelandic primary melts have near-uniform H_2O/Ce, despite having different initial H_2O and Ce contents. This interpretation is consistent with MORB data, which show that while there is significant global variation in H_2O/Ce, within individual regions H_2O/Ce remains approximately constant (Michael, 1995). Our data thus indicate that H_2O/Ce for Icelandic melts is best modelled with a constant value of $\sim 180 \pm 20$ which is insensitive to the degree of trace element enrichment in the primary melt. The effect of assuming variable source H_2O/Ce for enriched and depleted primary melts is explored in the supplementary information.

5.2. Diffusive loss and gain of H^+

Having estimated H_2O/Ce for EVZ primary melts, the Ce content of each melt inclusion or glass can be used as a proxy for its initial H_2O content. Measured Ce concentrations were used to predict initial H_2O concentrations for the EVZ inclusions and glasses (Fig. 6(a)). Melt inclusions and glasses with measured $H_2O/Ce = 180 \pm 20$ are considered to be unmodified and preserve the pre-eruptive melt H_2O content, which is 0.36 ± 0.03 wt% H_2O for Skuggafjöll and 0.57 ± 0.05 wt% H_2O for Laki. These values assume that there was no significant degassing of H_2O during magma ascent. Melt inclusions from Laki lava samples and Laki glasses have a wide range of predicted initial H_2O contents, but uniformly low measured H_2O of <0.1 wt%. The low H_2O of the Laki glass is explained by syn-eruptive H_2O degassing, which is thought to have been highly efficient: Thordarson et al. (1996) estimated that 70% of the total magmatic H_2O was released at the vents. Low H_2O in melt inclusions from Laki lava samples thus results from diffusive re-equilibration between these inclusions and the degassed lava during post-eruptive insulated transport.

Depleted inclusions from Laki and Skuggafjöll, and one enriched Laki inclusion with La/Yb = 6.1, have low predicted H_2O but high measured H_2O contents (Fig. 6(a)). This is explained by a process of over-hydration, whereby inclusions gain H^+ through diffusive equilibration with their carrier melt. 94% of inclusions from Skuggafjöll and 30% of inclusions from the Laki tephra appear to be over-hydrated in this manner. Over-hydrated Skuggafjöll inclusions have measured H_2O contents of 0.38 ± 0.02 wt%, identical to measured H_2O in the Skuggafjöll glass. Over-hydrated Laki inclusions contain 0.54 ± 0.09 H_2O, identical within error to unmodified Laki inclusions.

The over-hydrated EVZ inclusions preserve the pre-eruptive H_2O content of their carrier melts. This indicates that hydration occurs in the magma reservoir, prior to eruption, when olivines

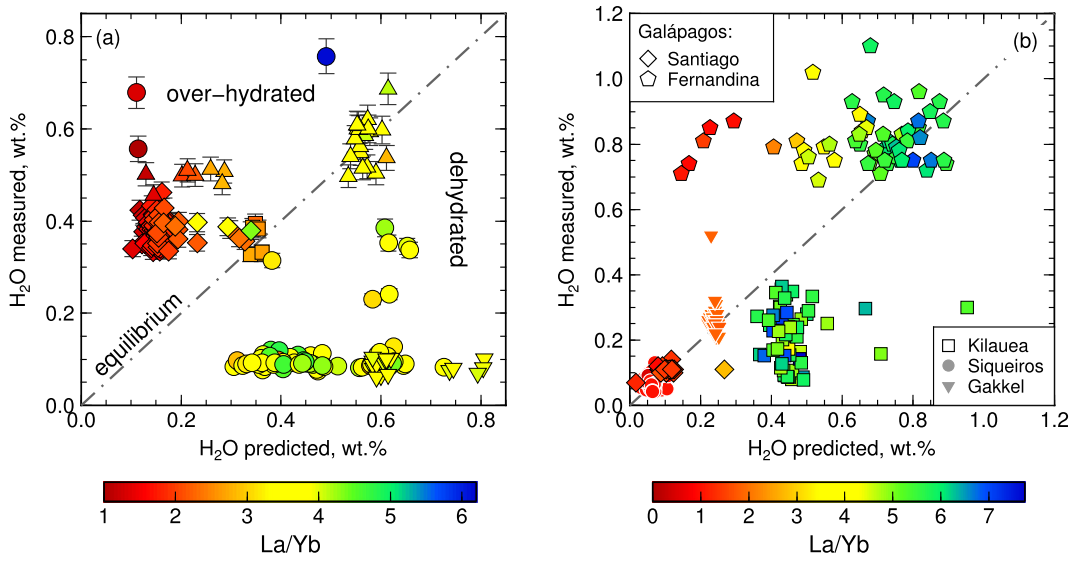

Fig. 6. (a) Predicted H_2O content of EVZ melt inclusions (calculated using the measured Ce content as a proxy for initial H_2O and assuming $H_2O/Ce = 180$) vs. measured H_2O content, coloured by La/Yb. Melt inclusions and glasses preserving the pre-eruptive melt H_2O content plot on the 'equilibrium' 1:1 line. Dehydrated melt inclusions and degassed glasses fall below the 1:1 line; melt inclusions that have gained H_2O through diffusive hydration plot above the 1:1 line. (b) Measured vs. predicted H_2O contents of melt inclusions from various global localities. The pattern of 'equilibrium', dehydrated/degassed and hydrated melt inclusions is evident in the global dataset, with the most depleted inclusions from any given eruption being the most hydrated. (For interpretation of the references to colour in this figure legend, the reader is referred to the web version of this article.)

containing melt inclusions with low initial H_2O contents are stirred into a more hydrous carrier melt. Over-hydration of depleted inclusions is therefore a predicted consequence of concurrent mixing and crystallisation of diverse primary melts. Diffusive over-hydration of Laki melt inclusions could not have occurred post-eruption, since the Laki melt degassed its H_2O very efficiently at the vents, and Laki magmatic tephra did not interact with external water (Thordarson et al., 1996). We also interpret the over-hydration of Skuggafjöll inclusions as a pre-eruptive process because Skuggafjöll glass has identical H_2O/Ce to unmodified melt inclusions from the Laki tephra, and there is no evidence of elevated H_2O concentrations in the Skuggafjöll glass, which would be expected if glacial water had been incorporated upon eruption. Hydration is most likely to have occurred within the Laki and Skuggafjöll magma chambers at the final depth of crystal-melt equilibration prior to eruption.

The most over-hydrated EVZ melt inclusions have gained up to 0.6 wt% H_2O (Fig. 6(a)). Addition of 0.6 wt% H_2O to an olivine-saturated basaltic melt results in a lowering of the olivine liquidus temperature by 23.3 °C (Médard and Grove, 2008). Reverse fractional crystallisation models of EVZ melt compositions suggest that, if the melt temperature were kept constant, the addition of 0.6 wt% H_2O would result in up to 3% dissolution of olivine at the melt inclusion walls. However, the EVZ inclusions have undergone on average ~2% post-entrapment crystallisation on the inclusion walls, which indicates that the rate of melt cooling balances or exceeds the rate of depression of the olivine liquidus that results from over-hydration of the melt inclusion. We find no visual or geochemical evidence for olivine dissolution into the EVZ melt inclusions.

5.3. Hydration of enriched and depleted inclusions

Diffusive hydration of melt inclusions will occur only if there are significant differences in H_2O activity, aH_2O, between melt inclusions and carrier melt (e.g. Qin et al., 1992; Gaetani et al., 2012). Water activity is dependent on pressure and, to a lesser extent, temperature (Burnham, 1979). Since the internal pressure in a melt inclusion, P_{int}, may differ from the external pressure P_{ext}, equilibrium H_2O concentrations of a melt inclusion and its carrier melt may differ (e.g. Qin et al., 1992). We investigated the range of potential aH_2O gradients between the EVZ inclusions and their carrier melts. Modelled melt inclusion compositions were selected to be representative of the most depleted and most enriched Laki and Skuggafjöll inclusions, with external melt compositions representative of the pre-eruptive Laki and Skuggafjöll carrier melts respectively (Table 1). Initial H_2O concentrations for the melt inclusions were calculated from measured Ce contents, assuming initial $H_2O/Ce = 180$.

There are considerable uncertainties in estimating melt inclusion P_{int}. If melt inclusions are assumed to behave as isochoric systems with $\Delta P/\Delta T$ equal to the ratio of the melt thermal expansion coefficient to its compressibility, then P_{int} is principally

Table 1
Compositions and radii of the most depleted and most enriched melt inclusions and their host olivines for Laki and Skuggafjöll, and their pre-eruptive carrier melt compositions. The melt compositions are the average tephra glass composition for Laki, and the average quenched pillow glass composition for Skuggafjöll. Data are from Hartley et al. (2014) and Neave et al. (2014a). 'H_2O meas' is the water content measured by SIMS; 'H_2O ini' is the estimated initial water content calculated from the given Ce concentrations and assuming $H_2O/Ce = 180$.

	Laki			Skuggafjöll		
	MI_{enr}	MI_{depl}	melt	MI_{enr}	MI_{depl}	melt
SiO_2, wt%	49.45	50.39	49.39	50.59	51.46	48.61
TiO_2	2.52	1.25	3.17	1.21	1.02	1.99
Al_2O_3	14.42	16.56	12.77	16.45	15.94	12.62
FeO	10.17	8.67	14.41	6.97	6.93	12.46
MnO	0.10	0.20	0.20	0.14	0.18	0.20
MgO	5.00	6.38	5.49	7.18	7.44	7.01
CaO	12.53	14.16	9.75	14.59	14.54	11.50
Na_2O	2.58	2.09	2.84	2.05	1.84	2.29
K_2O	0.50	0.06	0.50	0.16	0.10	0.22
P_2O_5	0.23	0.08	0.33	0.14	0.07	0.14
H_2O meas	0.76	0.56	0.08	0.40	0.42	0.36
H_2O ini	0.49	0.11	0.59	0.23	0.12	0.35
Fo, mol%	80.0	85.9		86.2	86.5	
Ce, ppm	27.3	6.3	33.0	12.9	6.5	19.5
La/Yb	6.1	1.0	3.8	3.4	1.2	2.6
r_{MI}, μm	25.4	24.0		96.4	47.2	
r_{ol}, μm	400	375		750	750	

controlled by temperature. Physical models can then be used to calculate internal pressure changes within an inclusion in response to decompression and cooling (e.g. Zhang, 1998). For basaltic melt inclusions trapped at high pressure, the percentage decrease in P_{int} in response to decompression and cooling is greater than for an inclusion trapped at intermediate or low pressure; however, inclusions trapped at higher pressure still maintain higher absolute P_{int} (e.g. Schiano and Bourdon, 1999 and references therein). Post-entrapment crystallisation has also been shown to raise P_{int} for H_2O-saturated inclusions or lower P_{int} for CO_2 or H_2O–CO_2-saturated inclusions (Steele-MacInnis et al., 2011). Despite these complexities, melt inclusion trapping pressures provide a useful upper estimate of P_{int}.

Melt inclusion trapping pressures can be estimated using CO_2–H_2O solubility models to calculate the volatile saturation pressure. The most enriched Laki melt inclusion contains 4767 ppm CO_2 and its calculated saturation pressure is 7.4 kbar (Hartley et al., 2014). Depleted Laki inclusions have CO_2 concentrations of 500–700 ppm and calculated saturation pressures of ~1.5 kbar. However, these inclusions are likely to have been trapped from vapour-undersaturated melts; thus the calculated saturation pressures provide only a minimum estimate of the depth of inclusion trapping. We therefore assume an average inclusion trapping pressure and temperature of 5 kbar and 1200 °C for enriched and depleted Laki inclusions, and an external pressure and temperature of 1.5 kbar and 1150 °C at the final stage of crystal-melt equilibration (Neave et al., 2013). Skuggafjöll melt inclusions are generally more depleted and have lower CO_2 contents than those from Laki, but evidence of CO_2 supersaturation in depleted Skuggafjöll inclusions (Neave et al., 2014a) means that calculated saturation pressures should be treated as maxima. We assume a pressure and temperature of 2 kbar and 1230 °C for Skuggafjöll inclusion trapping, and 0.5 kbar and 1190 °C for the final stage of crystal-melt equilibration (Neave et al., 2014a).

Water activities of melt inclusions and carrier melt were calculated following Burnham (1979) using the P-T conditions described above. Calculated aH_2O values for enriched and depleted Laki inclusions were 0.07 and 0.003 respectively; $aH_2O = 0.25$ for the Laki carrier melt. For Skuggafjöll, enriched and depleted inclusions had aH_2O of 0.02 and 0.01; the carrier melt had $aH_2O = 0.21$. In both cases, the water activity gradient is sufficient to promote H^+ diffusion into the melt inclusions (e.g. Portnyagin et al., 2008). If the inclusions are instead assumed to be trapped in a shallow magma reservoir, i.e. $P_{int} = P_{ext}$, the differences in aH_2O between inclusion and carrier melt are maintained for depleted inclusions but are somewhat reduced for enriched inclusions: at $P_{int} = P_{ext}$, $aH_2O = 0.15$ for the most enriched Laki inclusion and 0.06 for the most enriched Skuggafjöll inclusion.

The most enriched Laki melt inclusion has a high measured H_2O content of 0.76 wt%, and also appears to have undergone over-hydration (Fig. 6(a)). The high H_2O concentration and apparent hydration may reflect equilibration of this inclusion with an evolved mush liquid (Passmore et al., 2012) prior to entrainment of this olivine into the Laki carrier melt. Assuming an internal pressure of 2 kbar, then this inclusion has $aH_2O = 0.29$. This yields a difference in aH_2O of −0.04 between the inclusion and the Laki carrier melt. This activity gradient may be too small to promote H^+ diffusion from this inclusion, which could explain the retention of its high H_2O content. Enriched, vapour-saturated melt inclusions are more likely than depleted, vapour-undersaturated inclusions to experience a lowering of P_{int} in response to PEC and CO_2 exsolution into a vapour phase, and are therefore more likely than depleted inclusions to have aH_2O that is very similar to the external melt. The resultant low activity gradients mean that enriched inclusions are more likely to preserve unmodified H_2O contents and H_2O/Ce signatures, and may become dehydrated if there is a large negative activity gradient.

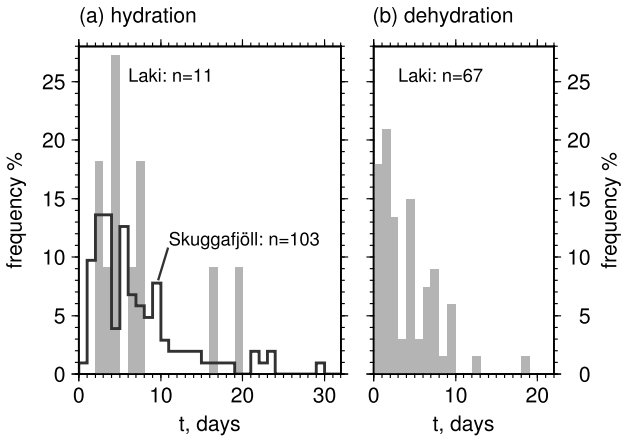

Fig. 7. Histograms showing calculated timescales of (a) diffusive hydration and (b) diffusive dehydration of EVZ melt inclusions. Laki is shown by grey solid bars; Skuggafjöll by the dark line.

Our calculations suggest that even when $P_{int} = P_{ext}$ there is a positive aH_2O gradient between a depleted melt inclusion and its carrier melt. Therefore, depleted inclusions are always expected to undergo diffusive hydration when mixed into more hydrous carrier melts. This is consistent with our observations. Over-hydration of depleted melt inclusions is therefore an inevitable consequence of concurrent mixing and crystallisation of diverse primary melts.

5.4. Timescales of diffusive over-hydration and dehydration

Timescales of diffusive equilibration of the EVZ melt inclusions with their carrier melts were calculated using a modified version of the model presented by Bucholz et al. (2013) to calculate an analytical solution for symmetric H^+ diffusion through a spherical olivine crystal hosting a spherical melt inclusion at its centre (Qin et al., 1992). Melt inclusion and olivine radii are provided in the supplementary material. We used a partition coefficient $D_{H_2O}^{olv\text{-}melt} = 0.0007$ (Le Voyer et al., 2014), which is assumed to be independent of pressure, temperature and melt H_2O content (Hauri et al., 2006). We assume isotropic diffusion of hydrogen and metal vacancies (V_{Me}) through the host olivine crystal, using the experimentally determined diffusion coefficients $D_{[001]}^{H^+} = 10^{-1.4}\exp[-(258/RT)]$ m^2/s (Demouchy and Mackwell, 2006) and $D_{V_{Me}} = 10^{-11.2}$ m^2/s (Wanamaker, 1994). Calculations were performed at pre-eruptive magmatic temperatures of 1190 °C for Skuggafjöll (Neave et al., 2014a) and 1140 °C for Laki (Guilbaud et al., 2007; Neave et al., 2013).

For each melt inclusion, initial H_2O contents were calculated using the measured Ce content assuming initial H_2O/Ce = 180. The Skuggafjöll carrier melt was assumed to contain 0.36 wt% H_2O; the Laki carrier melt was assumed to contain 0.57 wt% H_2O. We then calculated the timescale required for each of the EVZ inclusions to attain their measured H_2O contents via diffusive hydration. For Skuggafjöll melt inclusions the calculated timescales ranged from 0.83 to 29.2 days (Fig. 7(a)), with an average timescale of 7.1 ± 5.8 days (1σ). Timescales for the Laki inclusions ranged from 2.5 to 19.1 days (Fig. 7(a)), with an average of 7.3 ± 5.6 days (1σ). Complete re-equilibration between melt inclusions with low initial H_2O contents and their more hydrous carrier melts is achieved within days. This demonstrates that H_2O contents measured in rapidly quenched melt inclusions are primarily controlled by the extent of pre-eruptive diffusive re-equilibration between inclusions and carrier melt, rather than the H_2O content of the parental melt from which the inclusion was trapped.

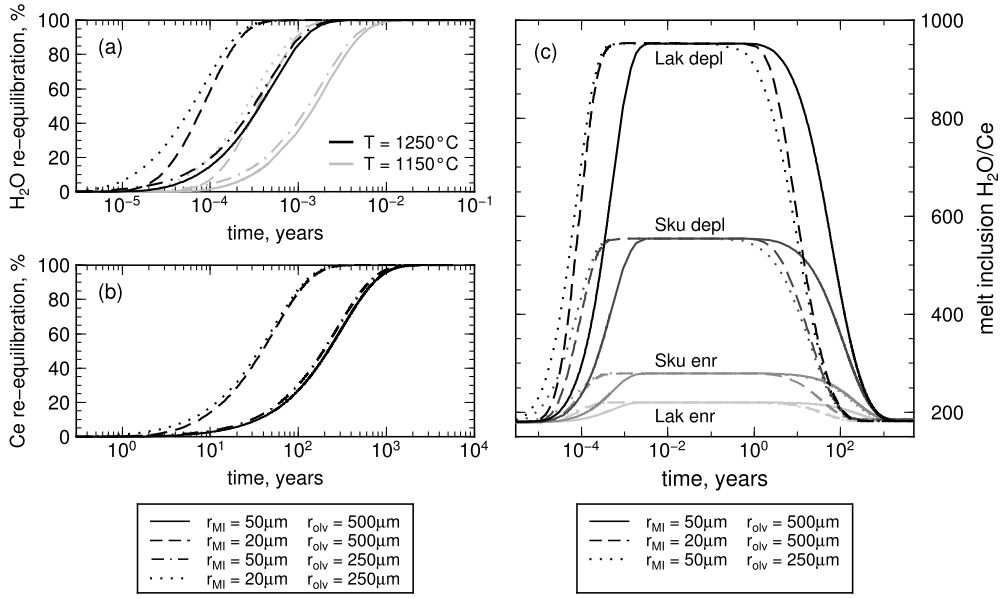

Fig. 8. Equilibration timescales for (a) H_2O and (b) Ce between olivine-hosted melt inclusions and carrier melt at 1250 °C, calculated using the model of Qin et al. (1992). Initial compositions represent the most depleted Laki melt inclusion and the pre-eruptive Laki carrier melt with compositions given in Table 1. Solid, dashed and dotted lines show the effect of varying melt inclusion and/or olivine radius. Grey lines in (a) show the effect of decreasing the temperature to 1150 °C on the rate of H^+ diffusion. (c) Evolution of H_2O/Ce in melt inclusions in response to simultaneous H_2O and Ce through the host olivine at 1250 °C. The four sets of curves represent the most enriched and most depleted melt inclusion compositions from Laki and Skuggafjöll, held in the Laki or Skuggafjöll pre-eruptive melt respectively, with compositions shown in Table 1. H_2O/Ce is assumed to be 180 at the time of inclusion trapping. The maximum H_2O/Ce reached within the inclusion is controlled by the difference in Ce concentrations between the inclusion and its carrier melt. Solid, dashed and dotted lines show the effect of varying melt inclusion and/or host olivine radius. Typical olivine-hosted melt inclusions can retain their maximum H_2O/Ce for 1–10 yr at magmatic temperatures, and are only restored to the 'equilibrium' value of 180 after 10^2–10^3 yr.

Some olivine-hosted inclusions from Laki lava samples also experienced post-eruptive H^+ loss as they re-equilibrated with the degassed Laki lava (0.08 wt% H_2O) during insulated transport at ~1120 °C (Guilbaud et al., 2007). We calculated the timescale required for melt inclusions with initial H_2O contents in equilibrium with the pre-eruptive Laki magma (0.57 ± 0.05 wt% H_2O) to reach their measured, dehydrated H_2O contents. In some cases the calculated timescale represents complete re-equilibration with the degassed Laki lava; in other cases the melt inclusions cooled below the closure temperature for H^+ diffusion before equilibrium was reached. The average calculated timescale for diffusive H^+ loss was 4.0 ± 3.4 days (Fig. 7(b)). The shortest dehydration timescale was 0.25 days for a melt inclusion with measured $H_2O = 0.352$ wt%, from a sample collected ~5 km from its source vent. The longest timescale was 18.3 days for an inclusion with measured $H_2O = 0.091$ wt%, from a sample collected ~30 km from its source vent. Laki lava surges advanced distances of 25–30 km from the vents over several days to a week; flow rates have been estimated at 6–7 and 15–17 km/day for the first two lava surges and 2–4 km/day for later surges (Thordarson and Self, 1993). The Laki lava samples considered in this study were collected at distances of ~5 km, ~15–16 km, ~22 km and ~29–30 km from their source vents (Fig. 1). The melt inclusions are therefore expected to have spent a minimum of <1 day up to ~15–20 days in insulated lava transport. Our calculated dehydration timescales are in good agreement with these estimates, which lends confidence to the use of H^+ diffusion as chronometer of post-eruptive processes.

5.5. Retention of non-equilibrium H_2O/Ce signatures

Rapid and complete H_2O equilibration between olivine-hosted melt inclusions and their external environment means that non-equilibrium high H_2O/Ce signatures may be achieved in a matter of hours to days. Diffusive equilibration of Ce between melt inclusions and an evolved carrier melt serves to lower H_2O/Ce within the inclusion. The retention of high H_2O/Ce signatures in melt inclusions is therefore dependent on the rate of Ce diffusion between inclusion and carrier melt.

Estimates of Ce diffusion coefficients in olivine at magmatic temperatures vary by several orders of magnitude, ranging from $D_{REE} \approx 10^{-15}$ m^2/s (Spandler et al., 2007; Spandler and O'Neill, 2010) to $D_{Ce} = 2.45 \times 10^{-20}$ m^2/s (Cherniak, 2010). Using these diffusion coefficients, a 50 μm radius melt inclusion in a 1 mm radius olivine equilibrates with its carrier melt in ~10^2 yr to >10^5 yr at 1300 °C. The reason for the discrepancies in diffusion coefficients between these studies is currently unclear. However, diffusion coefficients are partially controlled by the availability of suitable diffusion pathways which are in turn influenced by absolute elemental concentrations, as has been shown with respect to Li diffusion in olivine (Dohmen et al., 2010). Measured olivine REE concentrations were 1–10 ppm for the Spandler et al. (2007) and Spandler and O'Neill (2010) experiments, and up to 150 ppm in the Cherniak (2010) experiments. The Spandler et al. (2007) and Spandler and O'Neill (2010) experiments most closely reproduce the REE concentrations of the order 10–100 ppb expected for natural olivines (e.g. Beattie, 1994), suggesting that the faster diffusion coefficient may be most appropriate for natural systems (Qian et al., 2010).

Assuming fast REE diffusivity in olivine with $D_{REE} = 10^{-15.2}$ m^2/s (Spandler and O'Neill, 2010), a minimum constraint can be placed on the timescale over which Ce in olivine-hosted melt inclusions equilibrates with the external environment, and hence the timescale over which high H_2O/Ce can be preserved in melt inclusions at magmatic temperatures. We modelled the simultaneous diffusion of H and Ce from a spherical melt inclusion through a spherical olivine at 1250 °C, using the melt inclusion and carrier melt compositions given in Table 1. Our calculations demonstrate that even if Ce diffusion is assumed to be relatively fast, melt inclusions may retain the maximum H_2O/Ce signature for at least 10^0 years, and that H_2O/Ce is not restored to the equilibrium value until 10^2–10^3 yr have elapsed (Fig. 8).

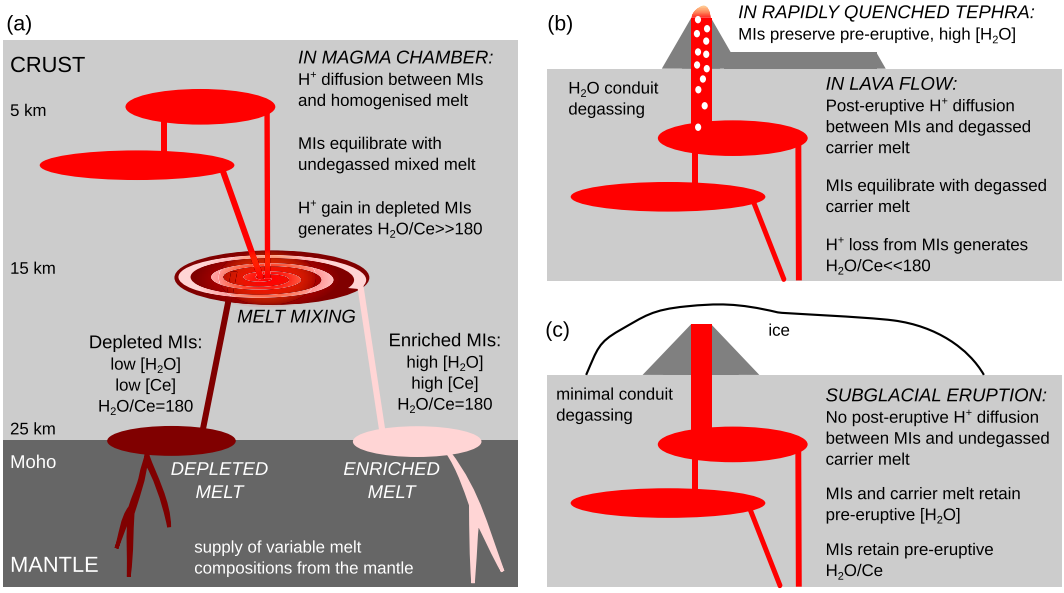

Fig. 9. Schematic illustration summarising the processes affecting H_2O/Ce in Icelandic magmatic systems. (a) Primary melts with variable trace element concentrations but uniform $H_2O/Ce \approx 180$ are supplied from the mantle. Melt inclusions (MI) trapped during crystallisation of depleted melts have low initial H_2O and Ce contents; inclusions trapped during crystallisation of enriched melts have high initial H_2O and Ce contents. Concurrent mixing and crystallisation produces a homogeneous carrier melt whose H_2O content is controlled by the proportions of enriched and depleted melts supplied to the mixture, and the extent of crystallisation. Melt inclusions diffusively equilibrate with this carrier melt. Depleted inclusions gain H^+, generating $H_2O/Ce \gg 180$. (b) Subaerial eruptions such as Laki degas much of their H_2O at the vents. Melt inclusions in rapidly quenched tephra are able to preserve their pre-eruptive H_2O contents. Inclusions in lava equilibrate with the degassed carrier melt during insulated transport, generating $H_2O/Ce \ll 180$. (c) Subglacial eruptions such as Skuggafjöll experience minimal H_2O degassing in the conduit, and are rapidly quenched upon eruption. Melt inclusions and glass both preserve their pre-eruptive H_2O contents.

5.6. Diffusive over-hydration recorded in global datasets

H_2O/Ce systematics can be used to predict initial H_2O contents for melt inclusions from any global locality, provided that H_2O/Ce for the primary melt can be determined. We calculated predicted H_2O contents for olivine-hosted inclusions from Siqueiros (Saal et al., 2002); the Gakkel Ridge (Shaw et al., 2010); Kilauea, Hawaii (Edmonds et al., 2013), and Santiago and Fernandina in the Gálapagos Islands (Koleszar et al., 2009) (Fig. 6(b)). Initial H_2O/Ce values used were 180 for Kilauea (Dixon and Clague, 2001); 193 for Gakkel (Shaw et al., 2010); 168 for Siqueiros (Saal et al., 2002); 117 for Santiago, and 250 for Fernandina (Koleszar et al., 2009).

As in the case of Iceland, the global data show that enriched melt inclusions are more likely to be dehydrated, while depleted inclusions are more likely to be over-hydrated. Owing to the higher Ce content of enriched melts and the fact that H_2O/Ce is not expected to vary between enriched and depleted primary melts, enriched melts are likely to dominate the H_2O budget of a mixed magma. The most enriched inclusions at any given locality thus record either 'equilibrium' H_2O contents or are slightly dehydrated, as is the case for Fernandina. The enriched Kilauea melt inclusions are degassed and perhaps also dehydrated through a process of convection, mixing, and exsolution of volatiles at low pressure (Edmonds et al., 2013).

For those locations where melt inclusions with a wide range in La/Yb have been recovered, the most depleted inclusions are the most over-hydrated, while more enriched inclusions preserve the unmodified H_2O content of the carrier melt. This is particularly evident for melt inclusions from Fernandina (Fig. 6(b)), where diffusive H^+ gain has strongly affected ~10% of the inclusions, and is attributed to the mixing and crystallisation of enriched and depleted mantle melts beneath the Gálapagos Islands (Koleszar et al., 2009). The large contrast in H_2O content and aH_2O between the depleted primary melts and the carrier melt promotes rapid hydration of the depleted melt inclusions.

Melt inclusions from Siqueiros, Gakkel and Santiago have near-identical La/Yb to matrix glass from these locations. The lack of trace element variability indicates either a lack of compositional diversity in the primary melts supplied to these magmatic systems, or that any mantle-derived compositional diversity was removed through mixing and homogenisation prior to melt inclusion trapping. In either case, melt inclusions and carrier melt will have similar aH_2O, leading to very limited diffusive H^+ exchange. A wide range of depleted and enriched melt inclusion compositions is therefore required in order to detect the effects of H^+ diffusion into and out of melt inclusions from any given eruption or locality.

In order for measured H_2O or H_2O/Ce to be used to infer the lithology, water content or melting history of the source mantle (e.g. Hauri et al., 2006; Bizimis and Peslier, 2015 and references therein), melt inclusion and glass compositions must be demonstrated to be representative of common primary melts. The Siqueiros, Gakkel and Santiago samples represent a best-case scenario whereby for each location, melt inclusions and glasses have near-identical trace element contents and ratios; both inclusions and glass were rapidly quenched and preserve the pre-eruptive H_2O content; and neither melt inclusion nor glass compositions appear to have been modified by mixing, degassing or diffusional processes. Measured H_2O and H_2O/Ce for these melts therefore provides a direct compositional link to the source mantle from which they were derived. Fernandina, Kilauea, and the EVZ are much more complex: for all these locations, melt inclusions have widely variable trace element contents and ratios indicative of concurrent mixing and crystallisation of diverse primary melts, and melt inclusions are variably hydrated or dehydrated depending on their compositions and their cooling histories. For Fernandina, Kilauea and Laki, the average matrix glass H_2O content is low, indicating syn-eruptive H_2O degassing. The combination of mixing, degassing and diffusion processes means that there is no simple relationship between measured H_2O and H_2O/Ce in these melt inclusions and glasses, and their mantle source. Melt water contents can be calculated using Ce as a proxy for H_2O, where H_2O/Ce for

the pre-eruptive, undegassed melts is determined from the compositions of rapidly quenched inclusions that have similar La/Yb to their carrier melt. This method is valid for any eruption provided that the melt inclusions have a genetic link to their carrier melt, which can be assumed if trace element ratios in the whole-rock and/or glass closely match the average melt inclusion composition (e.g. Maclennan, 2008). Trace element data are therefore vital for determining melt H_2O concentrations at the time of inclusion trapping, and ultimately the H_2O content of the mantle source.

6. Conclusions

We have used H_2O/Ce systematics to reconstruct the history of H^+ diffusion in olivine-hosted melt inclusions from Iceland's EVZ (Fig. 9). Trace element variability in these samples is best explained by the concurrent mixing and crystallisation of heterogeneous primary melt compositions. The distribution of H_2O contents is best explained by diffusive equilibration between the inclusions and their carrier melt, which is an inevitable consequence of concurrent mixing and crystallisation in magmatic systems. Enriched and depleted Icelandic primary melts are expected to have $H_2O/Ce \approx 180 \pm 20$. If olivine crystals hosting depleted melt inclusions with low initial H_2O and Ce contents are mixed into a more hydrous carrier melt, the inclusions will diffusively gain H^+ resulting in $H_2O/Ce \gg 180$. Diffusive hydration in the magma reservoir occurs prior to eruption on timescales of hours to days, and the resulting high H_2O/Ce values may be retained for up to 10^2–10^3 years at magmatic temperatures. Melt inclusions that are rapidly quenched upon eruption can preserve the H_2O content of their pre-eruptive carrier melt. Melt inclusions in crystals that spend hours to days in post-eruptive insulated lava transport preserve evidence of diffusive H^+ loss as the inclusions equilibrate with the degassed lava, resulting in $H_2O/Ce \ll 180$.

The effects of diffusive H^+ gain and loss are evident in global melt inclusion datasets. The signature of diffusive hydration is preserved almost exclusively in melt inclusions that are more depleted than their carrier melt. A range of enriched and depleted melt inclusion compositions is therefore required to detect the effects of pre-eruptive H^+ gain. Diffusive hydration of depleted melt inclusions is a predicted and inevitable consequence of concurrent mixing and crystallisation of diverse primary melts. Trace element data are therefore required to estimate the H_2O contents of melt inclusions at the time of inclusion trapping.

Acknowledgements

This work was supported by NERC grant NE/I012508/1 and a NERC studentship NE/1528277/1 to DAN. MEH acknowledges a Junior Research Fellowship from Murray Edwards College, Cambridge. We thank Anne Peslier and two anonymous reviewers for their thoughtful comments, and Bernard Marty for his editorial handling.

Appendix A. Supplementary material

Supplementary material related to this article can be found online at http://dx.doi.org/10.1016/j.epsl.2015.06.008.

References

Baker, D.R., Freda, C., Brooker, R.A., Scarlato, P., 2005. Volatile diffusion in silicate melts and its effects on melt inclusions. Ann. Geophys. 48, 699–717.

Beattie, P., 1994. Systematics and energetics of trace-element partitioning between olivine and silicate melts: implications for the nature of mineral/melt partitioning. Chem. Geol. 117, 57–71.

Bizimis, M., Peslier, A.H., 2015. Water in Hawaiian garnet pyroxenites: implications for water heterogeneity in the mantle. Chem. Geol. 397, 61–75.

Bucholz, C.E., Gaetani, G.A., Behn, M.D., Shimizu, N., 2013. Post-entrapment modification of volatiles and oxygen fugacity in olivine-hosted melt inclusions. Earth Planet. Sci. Lett. 374, 145–155.

Burnham, C.W., 1979. The importance of volatile constituents. In: Yoder, H.S. (Ed.), The Evolution of the Igneous Rocks: Fiftieth Anniversary Perspectives. Princeton University Press, pp. 439–482.

Chen, Y., Provost, A., Schiano, P., Cluzel, N., 2013. Magma ascent rate and initial water concentration inferred from diffusive water loss from olivine-hosted melt inclusions. Contrib. Mineral. Petrol. 165, 525–541.

Cherniak, D.J., 2010. REE diffusion in olivine. Am. Mineral. 95, 362–368.

Danyushevsky, L.V., 2001. The effect of small amounts of H_2O on crystallisation of mid-ocean ridge and backarc basin magmas. J. Volcanol. Geotherm. Res. 110, 265–280.

Danyushevsky, L.V., Della-Pasqua, F.N., Sokolov, S., 2000. Re-equilibration of melt inclusions trapped by magnesian olivine phenocrysts from subduction-related magmas: petrological implications. Contrib. Mineral. Petrol. 138, 68–83.

Danyushevsky, L.V., McNeill, A.W., Sobolev, A.V., 2002. Experimental and petrological studies of melt inclusions in phenocrysts from mantle-derived magmas: an overview of techniques, advantages and complications. Chem. Geol. 183, 5–24.

Danyushevsky, L.V., Perfit, M.R., Eggins, S.M., Falloon, T.J., 2003. Crustal origin for coupled 'ultra-depleted' and 'plagioclase' signatures in MORB olivine-hosted melt inclusions: evidence from the Siqueiros transform fault, East Pacific rise. Contrib. Mineral. Petrol. 144, 619–637.

Danyushevsky, L.V., Plechov, P., 2011. Petrolog3: integrated software for modeling crystallization processes. Geochem. Geophys. Geosyst. 12, 1–32.

Demouchy, S., Mackwell, S., 2006. Mechanisms of hydrogen incorporation and diffusion in iron-bearing olivine. Phys. Chem. Miner. 33, 347–355.

Dixon, J.E., Clague, D.A., 2001. Volatiles in basaltic glasses from Loihi Seamount, Hawaii: evidence for a relatively dry plume component. J. Petrol. 42, 627–654.

Dohmen, R., Kasemann, S.A., Coogan, L., Chakraborty, S., 2010. Diffusion of Li in olivine. Part I: experimental observations and a multi species diffusion model. Geochim. Cosmochim. Acta 74, 274–292.

Edmonds, M., Sides, I.R., Swanson, D.A., Werner, C., Martin, R.S., Mather, T.A., Herd, R.A., Jones, R.L., Mead, M.I., Sawyer, G., Roberts, T.J., Sutton, A.J., Elias, T., 2013. Magma storage, transport and degassing during the 2008–10 summit eruption at Kilauea Volcano, Hawaii. Geochim. Cosmochim. Acta 123, 284–301.

Elthon, D., Casey, J.F., 1985. The very depleted nature of certain primary mid-ocean ridge basalts. Geochim. Cosmochim. Acta 49, 289–298.

Faure, F., Schiano, P., 2005. Experimental investigation of equilibration conditions during forsterite growth and melt inclusion formation. Earth Planet. Sci. Lett. 236, 882–898.

Gaetani, G.A., O'Leary, J.A., Shimizu, N., Bucholz, C.E., Newville, M., 2012. Rapid reequilibration of H_2O and oxygen fugacity in olivine-hosted melt inclusions. Geology 40, 915–918.

Guilbaud, M.N., Blake, S., Thordarson, T., Self, S., 2007. Role of syn-eruptive cooling and degassing on textures of lavas from the AD 1783–1784 Laki eruption, south Iceland. J. Petrol. 48, 1265–1294.

Gurenko, A.A., Chaussidon, M., 1995. Enriched and depleted primitive melts included in olivine from Icelandic tholeiites: origin by continuous melting of a single mantle column. Geochim. Cosmochim. Acta 59, 2905–2917.

Gurenko, A.A., Chaussidon, M., 1997. Boron concentrations and isotopic composition of the Icelandic mantle: evidence from glass inclusions in olivine. Chem. Geol. 135, 21–34.

Gurenko, A.A., Chaussidon, M., 2002. Oxygen isotope variations in primitive tholeiites of Iceland: evidence from a SIMS study of glass inclusions, olivine phenocrysts and pillow rim glasses. Earth Planet. Sci. Lett. 205, 63–79.

Hartley, M.E., Maclennan, J., Edmonds, M., Thordarson, T., 2014. Reconstructing the deep CO_2 degassing behaviour of large basaltic fissure eruptions. Earth Planet. Sci. Lett. 393, 120–131.

Hartley, M.E., Thordarson, T., 2013. The 1874–76 volcano-tectonic episode at Askja, North Iceland: lateral flow revisited. Geochem. Geophys. Geosyst. 14, 2286–2309.

Hauri, E.H., Gaetani, G.A., Green, T.H., 2006. Partitioning of water during melting of the Earth's upper mantle at H_2O-undersaturated conditions. Earth Planet. Sci. Lett. 248, 715–734.

Koleszar, A.M., Saal, A.E., Hauri, E.H., Nagle, A.N., Liang, Y., Kurz, M.D., 2009. The volatile contents of the Galapagos plume; evidence for H_2O and F open system behavior in melt inclusions. Earth Planet. Sci. Lett. 287, 442–452.

Kuzmin, D.V., Sobolev, A.V., 2004. Boundary layer contribution to the composition of melt inclusions in olivine. Geochim. Cosmochim. Acta 68, A544.

Le Voyer, M., Asimow, P.D., Mosenfelder, J.L., Guan, Y., Wallace, P.J., Schiano, P., Stopler, E., Eiler, J., 2014. Zonation of H_2O and F concentrations around melt inclusions in olivines. J. Petrol. 55, 685–707.

Lloyd, A.S., Plank, T., Ruprecht, P., Hauri, E.H., Rose, W., 2013. Volatile loss from melt inclusions in pyroclasts of differing sizes. Contrib. Mineral. Petrol. 165, 129–153.

Mackwell, S.J., Kohlstedt, D.L., 1990. Diffusion of hydrogen in olivine: implications for water in the mantle. J. Geophys. Res., Solid Earth 95, 5079–5088.

Maclennan, J., 2008. Concurrent mixing and cooling of melts under Iceland. J. Petrol. 49, 1931–1953.

Maclennan, J., McKenzie, D., Grönvold, K., Shimizu, N., Eiler, J.M., Kitchen, N., 2003a. Melt mixing and crystallization under Theistareykir, northeast Iceland. Geochem. Geophys. Geosyst. 4, 8624.

Maclennan, J., McKenzie, D., Hilton, F., Grönvold, K., Shimizu, N., 2003b. Geochemical variability in a single flow from northern Iceland. J. Geophys. Res. 108, 2007.

Massare, D., Métrich, N., Clocchiatti, R., 2002. High-temperature experiments on silicate melt inclusions in olivine at 1 atm: inference on temperatures of homogenization and H_2O concentrations. Chem. Geol. 183, 87–98.

Médard, E., Grove, T.L., 2008. The effect of H_2O on the olivine liquidus of basaltic melts: experiments and thermodynamic models. Contrib. Mineral. Petrol. 155, 417–432.

Métrich, N., Sigurdsson, H., Meyer, P.S., Devine, J.D., 1991. The 1783 Lakagigar eruption in Iceland – geochemistry, CO_2 and sulfur degassing. Contrib. Mineral. Petrol. 107, 435–447.

Métrich, N., Wallace, P.J., 2008. Volatile abundances in basaltic magmas and their degassing paths tracked by melt inclusions. Rev. Mineral. Geochem. 69, 363–402.

Michael, P.J., 1995. Regionally distinctive sources of depleted MORB: evidence from trace elements and H_2O. Earth Planet. Sci. Lett. 131, 301–320.

Naumov, V.B., Dorofeeva, V.A., Girnis, A.V., Yarmolyuk, V.V., 2014. Comparison of major, volatile, and trace element contents in the melts of mid-ocean ridges on the basis of data on inclusions in minerals and quenched glasses of rocks. Geochem. Int. 52, 347–364.

Neave, D.A., Maclennan, J., Edmonds, M., Thordarson, T., 2014a. Melt mixing causes negative correlation of trace element enrichment and CO_2 content prior to an Icelandic eruption. Earth Planet. Sci. Lett. 400, 272–283.

Neave, D.A., Maclennan, J., Hartley, M.E., Edmonds, M., Thordarson, T., 2014b. Crystal storage and transfer in basaltic systems: the Skuggafjöll eruption, Iceland. J. Petrol. 55, 2311–2346.

Neave, D.A., Passmore, E., Maclennan, J., Fitton, G., Thordarson, T., 2013. Crystal-melt relationships and the record of deep mixing and crystallization in the AD 1783 Laki eruption, Iceland. J. Petrol. 54, 1661–1690.

Newcombe, M.E., Fabbrizio, A., Zhang, Y., Ma, C., Le Voyer, M., Guan, Y., Eiler, J.M., Saal, A.E., Stolper, E.M., 2014. Chemical zonation in olivine-hosted melt inclusions. Contrib. Mineral. Petrol. 168, 1–26.

Nichols, A.R.L., Carroll, M.R., Hóskuldsson, A., 2002. Is the Iceland hot spot also wet? Evidence from the water contents of undegassed submarine and subglacial pillow basalts. Earth Planet. Sci. Lett. 202, 77–87.

Padrón-Navarta, J.A., Hermann, J., O'Neill, H.S.C., 2014. Site-specific hydrogen diffusion rates in forsterite. Earth Planet. Sci. Lett. 392, 100–112.

Passmore, E., Maclennan, J., Fitton, G., Thordarson, T., 2012. Mush disaggregation in basaltic magma chambers: evidence from the AD 1783 Laki eruption. J. Petrol. 53, 2593–2623.

Peslier, A.H., Bizimis, M., Matney, M., 2015. Water disequilibrium in olivines from Hawaiian peridotites: recent metasomatism, H diffusion and magma ascent rates. Geochim. Cosmochim. Acta 154, 98–117.

Portnyagin, M., Almeev, R., Matveev, S., Holtz, F., 2008. Experimental evidence for rapid water exchange between melt inclusions in olivine and host magma. Earth Planet. Sci. Lett. 272, 541–552.

Qian, Q., O'Neill, H.S.C., Hermann, J., 2010. Comparative diffusion coefficients of major and trace elements in olivine at ~950 °C from a xenocryst included in dioritic magma. Geology 38, 331–334.

Qin, Z., Lu, F., Anderson, A.T., 1992. Diffusive reequilibration of melt and fluid inclusions. Am. Mineral. 77, 565–576.

Rosenthal, A., Hauri, E.H., Hirschmann, M.M., 2015. Experimental determination of C, F, and H partitioning between mantle minerals and carbonated basalt, CO_2/Ba and CO_2/Nb systematics of partial melting, and the CO_2 contents of basaltic source regions. Earth Planet. Sci. Lett. 412, 77–87.

Rudge, J.F., Maclennan, J., Stracke, A., 2013. The geochemical consequences of mixing melts from a heterogeneous mantle. Geochim. Cosmochim. Acta 114, 112–143.

Saal, A.E., Hauri, E.H., Langmuir, C.H., Perfit, M.R., 2002. Vapour undersaturation in primitive mid-ocean-ridge basalt and the volatile content of Earth's upper mantle. Nature 419, 451–455.

Schiano, P., Bourdon, B., 1999. On the preservation of mantle information in ultramafic nodules: glass inclusions within minerals versus interstitial glasses. Earth Planet. Sci. Lett. 169, 173–188.

Shaw, A.M., Behn, M.D., Humphris, S.E., Sohn, R.A., Gregg, P.M., 2010. Deep pooling of low degree melts and volatile fluxes at the 85°E segment of the Gakkel Ridge: evidence from olivine-hosted melt inclusions and glasses. Earth Planet. Sci. Lett. 289, 311–322.

Shorttle, O., Maclennan, J., 2011. Compositional trends of Icelandic basalts: implications for short-length scale lithological heterogeneity in mantle plumes. Geochem. Geophys. Geosyst. 12, Q11008.

Slater, L., McKenzie, D., Grönvold, K., Shimizu, N., 2001. Melt generation and movement beneath Theistareykir, NE Iceland. J. Petrol. 42, 321–354.

Spandler, C., O'Neill, H.S.C., 2010. Diffusion and partition coefficients of minor and trace elements in San Carlos olivine at 1300 °C with some geochemical implications. Contrib. Mineral. Petrol. 159, 791–818.

Spandler, C., O'Neill, H.S.C., Kamenetsky, V.S., 2007. Survival times of anomalous melt inclusions from element diffusion in olivine and chromite. Nature 447, 303–306.

Steele-MacInnis, M., Esposito, R., Bodnar, R.J., 2011. Thermodynamic model for the effect of post-entrapment crystallization on the H_2O–CO_2 systematics of vapor-saturated, silicate melt inclusions. J. Petrol. 52, 2461–2482.

Thordarson, T., Self, S., 1993. The Laki (Skaftár Fires) and Grímsvötn eruptions in 1783–1785. Bull. Volcanol. 55, 233–263.

Thordarson, T., Self, S., Óskarsson, N., Hulsebosch, T., 1996. Sulfur, chlorine, and fluorine degassing and atmospheric loading by the 1783–1784 AD Laki (Skaftár fires) eruption in Iceland. Bull. Volcanol. 58, 205–225.

Toplis, M.J., 2005. The thermodynamics of iron and magnesium partitioning between olivine and liquid: criteria for assessing and predicting equilibrium in natural and experimental systems. Contrib. Mineral. Petrol. 149, 22–39.

Wanamaker, B.J., 1994. Point defect diffusivites in San Carlos olivine derived from reequilibration of electrical conductivity following changes in oxygen fugacity. Geophys. Res. Lett. 21, 21–24.

Zhang, Y., 1998. Mechanical and phase equilibria in inclusion-host systems. Earth Planet. Sci. Lett. 157, 209–222.

Zhang, Y., Ni, H., 2010. Diffusion of H, C, and O components in silicate melts. Rev. Mineral. Geochem. 72, 171–225.

Zhang, Y., Ni, H., Chen, Y., 2010. Diffusion data in silicate melts. Rev. Mineral. Geochem. 72, 311–408.